Potential mineral occurrences from airborne geophysical and satellite image data, case study in Asir terrane, Arabian Shield

Taher Zouaghi[1, 2]

[1]Geoexploration Department, Faculty of Earth Sciences, King Abdulaziz University, Jeddah 21589, Saudi Arabia
[2]Laboratoire de Géoressources, CERTE, Pôle Technologique de Borj Cédria, Soliman 8020, Tunisia

---

Abstract:*Deep geometry and structuring of several areas of the Arabian Shield remain quite speculative since the scarcity of geophysical studies. N-trending structures that characterize the Asir terrane show a potential mineralization related to its tectonic setting and kinematic evolution. The Umm Farwah fault system and neighboring zones reveal many occurrences.*

Based on the integration of the aeromagnetic data, remote sensing, and geological data on the Biljurshi region, this work contributes to the understanding the geometrical relation of the Baish, Bahah and Jiddah syn-amalgamation sedimentary and volcanic structures, and of the Ablah post-amalgamation sedimentary and volcanic basin. It highlights the structural framework of the Umm Farwahshear zoneand its relationship with sedimentary, volcanic and metamorphic rocks and the associated plutonic and volcanic intrusions related to the major events that marked the Arabian Shield.

The airborne geophysical magnetic enhancement, assisted by satellite image analyses, coupled with field data, provide new application that confirms and improves the existing map and highlightsnew features in the Biljurshi area. The detailed investigation into local and regional structural setting of the Biljurshi area revealed the presence of a principal near N-S (N-S, NNE-SSW and NNW-SSE) lineaments, with minor NE-SW and NW-SE trending lineaments. Regional near N-S and those NNE-SSW and NNW-SSE secant lineaments or shear zones couldconsidered as possible pathways for migrating mineralized fluids.

Key Words:*Biljurshi; Magnetic filtering; Satellite image; Lineaments; Mineral potential*

Date of Submission: 13-04-2020   Date of Acceptance: 28-04-2020

I.   Introduction

Late Neoproterozoic N-trending reactivated features [1,2,3,4] mark the Asir terrane that is a part of the Arabian Shield (Figure 1). The Umm Farwah dextral strike-slip post-dated the Ablah group rhyolite eruption (640–613 Ma) [5,6]. Thrusts and shear zones master intra-terrane divide the Asir terrane into differential and complicated structural belts [7,8]; they may coincide with sutures that separate the sub-terranes. However, original relationships between these sub-terranes remain indistinguishable [4,9,10]. N-S trending polyphase master strike slip faults and structures, which are connected to other second order faults in the Biljurshi study area (Figure 2), could be linked to the tectono-magmatic events [7,10,11,12,13]. The deep structure of the Ablah group belt and its relationship with the Umm Farwah shear zone in the Biljurshi area need more detailed study.

The Biljurshi area hosts several ancient mines and prospect zones; slag piles and veins were identified [11,12]. Mineral deposition could be syngenetic and parallel to foliation or epigenetic along fractured zones and essentially contains immense fluorite and veins, and pods of Cu-, Pb-, Zn-, and Ag-sulfides in a breccia's pipe [11,12,14,15]. The different mining camps were highlighted for economic substances. Structural control is evident by the alignment of indices and mines along some deformation corridors in the study area. Sometimes, the distribution of basic metals as indices or mines does not show a direct relationship with the localization of the faults. This distribution suggests that this type of mineralization is controlled more by the characteristics of volcanism (syngenetic) than by the structural elements. In this work, we try to propose some mineral potential zones based on the obtained structural models.

II.   Geology

The Umm Farwah N-S trending shear zone (Figures 1 and 2) is the major structure that runs through the Biljurshi area. This fault systemis characterized by N-S trending linear belts and structures of intense ductile deformations, associated with serpentine and talc schist bodies [11,12]. Most authors believe that these linear belts of intense deformation are relicts of faulting, and therefore refer to them as shear zones [10,11,16]. The N-oriented master Umm Farwah fault (Figures 1 and 2) crosses the Asir terrane and seems hosted in early Cryogenian volcano-sedimentary and plutonic rocks [15,17]. [17] highlights a typical A-type granitoids of the

---

Ablah-Shuwas pluton. Emplacement of the discontinuous ring complexes and irregular bodies seems to be related to movement of the Umm Farwah shear zone during the Ediacaran period (about -610 Ma age or later). Strike-slip rejuvenations of the Umm Farwah deep-seated fault system, during the Ediacaran period (about -610 Ma age or later), caused partial melting and rising of mantle flux, and crustal fusion in the arc-related lower mafic and upper volcano-plutonic crust of intermediate to felsic compositions producing A-type granitoids [17]. S–C fabrics of this fault suggest both dextral and sinistral movements [15]. Nevertheless, its absolute motion is still unknown.

The Ablah marine sedimentary and volcanic molassic syncline (640–615 Ma) [15,18], located along the N-S Umm Farwah master fault (Figure 2), was deposited at time of and soon after the Nabitah orogeny (680–640 Ma) [15]. This post-amalgamation basin marked by unconformities that followed the successive tectonic events of the basement, indicating its formation during the crustal deformations [15,18].
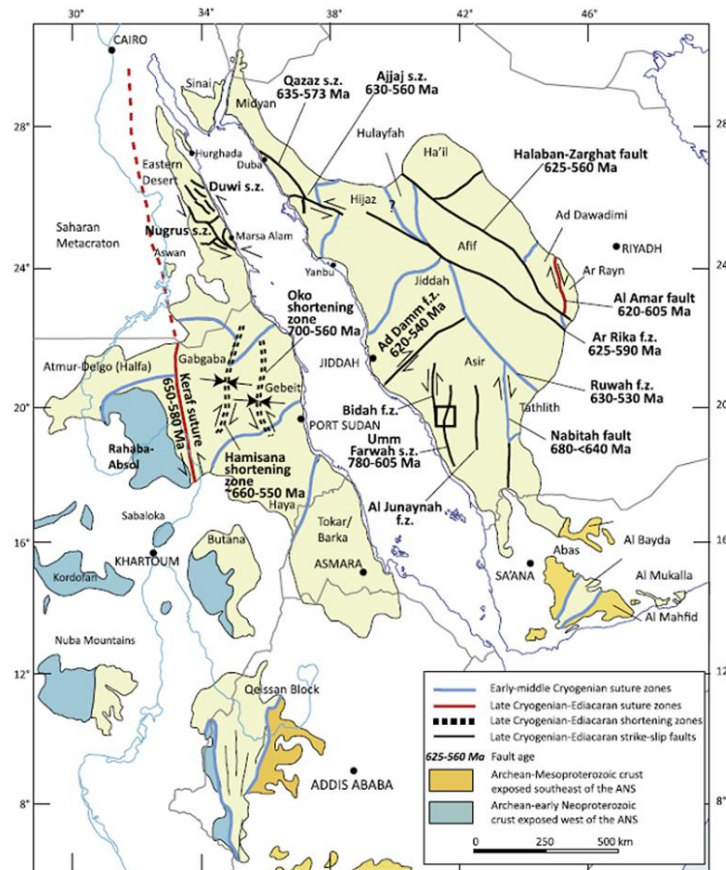

Figure 1. Regional structural map of the Arabian-Nubian Shields [15].

The Biljurshi area (Figure 1), situated at the center of the Neoproterozoic Asir Terrane, shows typical intra-terrane features. The formation of these features in Arabian Shield believed to be a result major movement within the crust. This area displays lithology that is typical of the Neoproterozoic in the Arabian Shield, namely different types of igneous rocks like diorite/gabbro complexes, and granodiorites [16,19]. Two types of Precambrian rocks mark the Biljurshi area, volcanic, sedimentary and metamorphic rocks formed Baish, Bahah, Jiddah and Ablah groups, and plutonic and volcanic intrusions [11,12,15].

III. Material and methods

3.1. Aeromagnetic

Lockwood Survey Corp., Ltd.; Aero Service Corp.; Hunting Geology and Geophysics, Ltd.; and the Arabian Geophysical and Surveying Company made the airborne geophysical survey. The aeromagnetic data were recorded along northeast-southwest flight lines, which are spaced 0.5 mile (0.8 km) apart 300 ft (91.5 m) above land surface [11]. The high topographic relief in the southwest part of the quadrangle impose an approximately a northwest-southeast diagonal line delineation of the quadrangle and, therefore, apoor magnetic continuity is obtained along certain portions of the joining areas [11]. There are no data above too high relief because limits prescribed by flight specifications. A linear gradient, which includes corrections for diurnal variations and instrument drift, was removed from the observed profile data along the flight path. This gradient

is not precisely known but it approximates the earth's main field. The International Geomagnetic Reference Field (IGRF) for the Biljurshi area was removed.
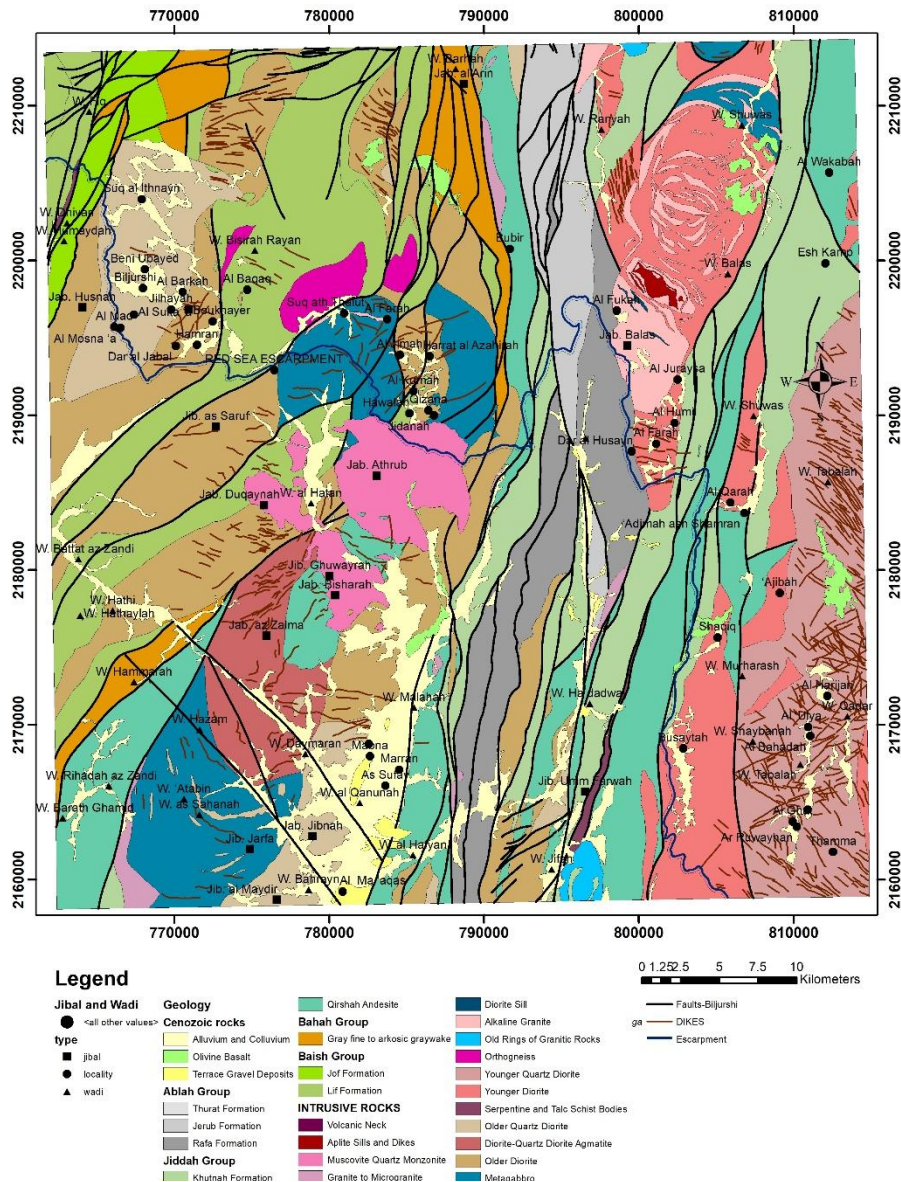

Figure 2. Field exposed rocks and faults map of the Biljurshi area [11], displaying the predominant north-south oriented rock bodies and tectonic features.

The Fourier transforms that become common practice in geophysics, have been demonstrated since the sixties [20,21,22,23,24]. Indeed, the magnetic field can be represented exactly by a development in Fourier series, used to calculate the different transformations applied to the magnetic data [25].Various mathematical operators of transformation are used to manipulate the magnetic grid maps in order to obtain the maximum information. The transformed maps (reduction to the pole, vertical gradient, and horizontal gradient magnitude) by each operator are presented. Theestablished lineaments map summarize all interpretations of the aeromagnetic transformed maps, satellite images and outcropping geology.

3.2. Landsat image

Extraction operations were applied on Landsat ETM images. Band 5 of a spatial resolution 30*30 meter was chosen for automated extraction of lineaments. This band was selected among the others because it is useful in the distinction of lineaments and other geological features; this band is also sensitive to the moisture content of the vegetation [26].

The methodological approach followed in this study involves three steps. The first step consists of selecting the image to be processed, among images produced combinations of the bands, by comparing the

lineaments with these extracted from the fracturing images recorded on a geological map. The second step is reserved for the extraction and validation of discontinuities extracted from the image. The last step is devoted to the statistical study of the obtained lineaments and their comparison with the fault map and outcropping rocks. This will allow us to deduce their genesis and their role in the tectonic kinematics of the region.

IV. Results

4.1. Geophysical lineaments
4.1.1. *Reduce to pole (RTP)*

The magnetic anomalies reduced to the pole coincide with some geological structures composed of basement rocks that characterize the Arabian Shield and which are part of the volcanic complex of the Asir terrane (Figure3). Accordingly, changes in the magnetic field should be generated by the contrast of susceptibility between the mafic and intermediate rocks, and the acidic (granitic) and metamorphic (meta-volcanic and meta-sedimentary) rocks.

Figure 3. Reduce to pole (RTP) map of the Biljurshi area,displaying the magnetic anomalies.

The pole-reduced magnetic anomaly map shows a clear correspondence between the higher amplitude magnetic anomalies and exposed intrusive mafic rocks. In the obtained maps the geological structures are more clearly expressed, i.e., the distribution of the meta-volcano-sedimentary structures, the distribution of intrusive igneous rocks and the uplifts of the basement rock. The identified anomalies can be subdivided into several domains that are substantially superimposed on different Precambrian structures of the study area. Roughly, the RTP map shows areas of relatively distinct anomalies (Figure 3). It can be subdivided into areas of positive anomalies (Zone of Al Farah-Jabal Balas-Wadi Shuwas, Zone of Jabal al-Arin-Wadi Bisarah Rayan-Al Kumah, Zone at western edge of the Ablah group belt, Zone of Busaytah-Ajibah, and Zone of the Jibal Jarfa-Wadi Rihadah az Zandi), and areas of negative anomalies, mainly well highlighted westward the study area.

4.1.2. *Magnetic gradient*

The first vertical derivation map shows a perfect correlation with the geology in outcrop (Figure 4). The anomalies of the vertical gradient map show variable size, shape and amplitude. The anomaly zones, which highlight N-oriented major featureson the RTP maps, reveal anomalies of small dimensions and multiple directions (Figure 4). These anomalies are, thus related to superficial sources, arranged in corteges aligned in different directions but with varying proportions. The anomaly zones highlight major features most of which are N-S on the RTP map. They reveal anomalies of small dimensions and multiple directions (Figure 4). The domains of anomalies defined on the reduced to pole map show a high gradient on the vertical derivative map by molding on its sides. The gradient variation corresponds to discontinuities interpreted as lithological contacts. Some of these contacts are associated with faults, which intersect them, in most cases longitudinally, at their borders.
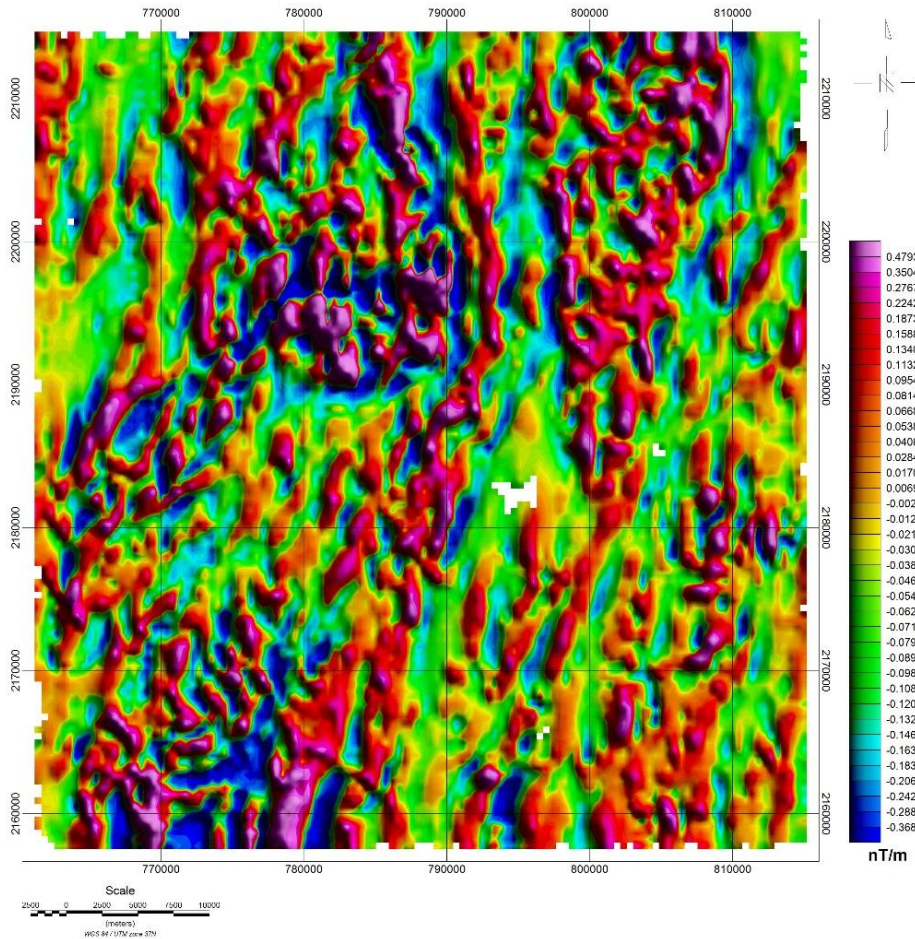
Figure 4. First vertical gradient (derivative) map of the Biljurshi area.

The horizontal gradient operator applied to the magnetic intensity field reduced to the pole allowed determination of linear anomalyin the Biljurshi region (Figure 5). We notice that the horizontal gradient provides a more appreciable picture. N-trending features dominate the horizontal gradient magnitude map of the RTP; they coincide with the Ablah basin crossed by the Umm Farwah shear zone. The obtained gradient aligned in different directions reflects the location of rock contacts and faults (Figure 5).
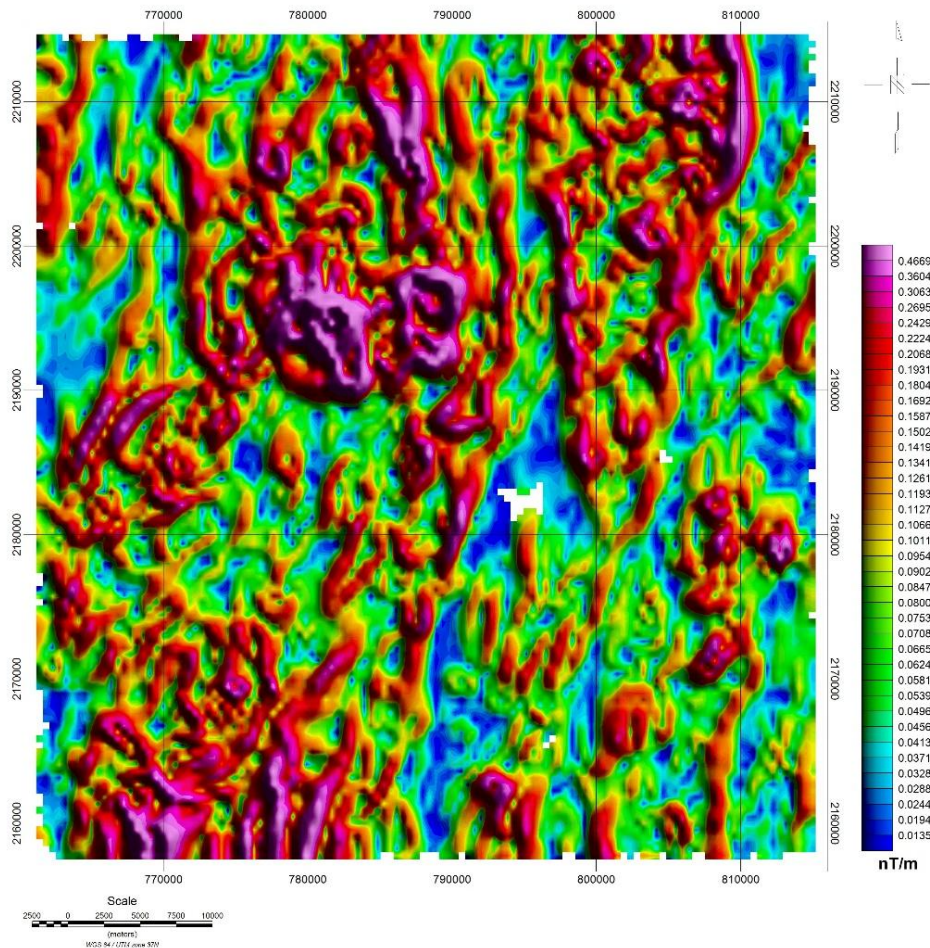
Figure 5. Horizontal gradient magnitude (HGM) of the Biljurshi area.

4.2.   Satellite image lineaments
4.2.1. Lineaments map

The synthesis map of lineaments represents a set of unique segments resulting from the processed image of the Biljurshi study region (Figure 6). The lineaments vary from hectometric to plurikilometric in length. Directions highlightedare close to N-S, NNE-SSW to NE-SW and NNW-SSE. A few linear elements form fine close-up frames oriented generally in the same direction forming thus swarms of lineaments. The analysis of rose diagramsin frequency and length reveals the main following categories(Figure 6): high proportion of lineaments (N-S to NNE-SSW (N0-10)); medium proportion of lineaments (NNE-SSW to NE-SW (N10-40) and NNW-SSE (N150-180)); small proportions (NE-SW (N40-70) and NW-SE (N120-150); and very small proportion (WNW-ESE (N90-120)).

4.2.2. Density map

The lineament density map reveals high, medium, and devoid zones (Figure 6). N-S to NNE-SSW are the dominated faults zones. Lowest density is highlighted westward.The N-oriented Umm Farwah Fault Zone (UFFZ), that crosses the volcano-sedimentary the Ablah group belt, is associated with higher density zones(Figure 6). A second fault zone extends from jibal Umm Farwah to the south and elongates along a NNE-SSW direction, delimiting intrusive bodies of Al Farah-Al Juraysa-Al Fukah domain. In fact, this fault zone is part of the Umm Frawah master system. Another fault zone of high-density and of NW-SE direction is also demonstrated in neighborings of the Umm Farwah major fault system. This system connects the metagabbro complex of Suq ath Thalut-Al Kumah in the northwest with the Ablah highly faulted basin. It intersects intrusive rocks, especially the muscovite quartz monzonite of Jabal Athrub. Other minor (shorter) fault zones of high density area highlighted on the density map. Northward, a N-S faulting zone is showed in the Wadi Dhiyan-Wadi Fiq; the other of NE-SW orientation located to the west of the Umm Farwah shear zone at the level of the Lif formation (Figure 6). The N-S high density zone was also highlighted over younger diorite of the Busaytah area in the southeast part of the map. Further zones of high density are showed in the southeast part of the map; the most differentiated of N-S direction is located at the Wadi Barath Ghamid Qirshah andesite.
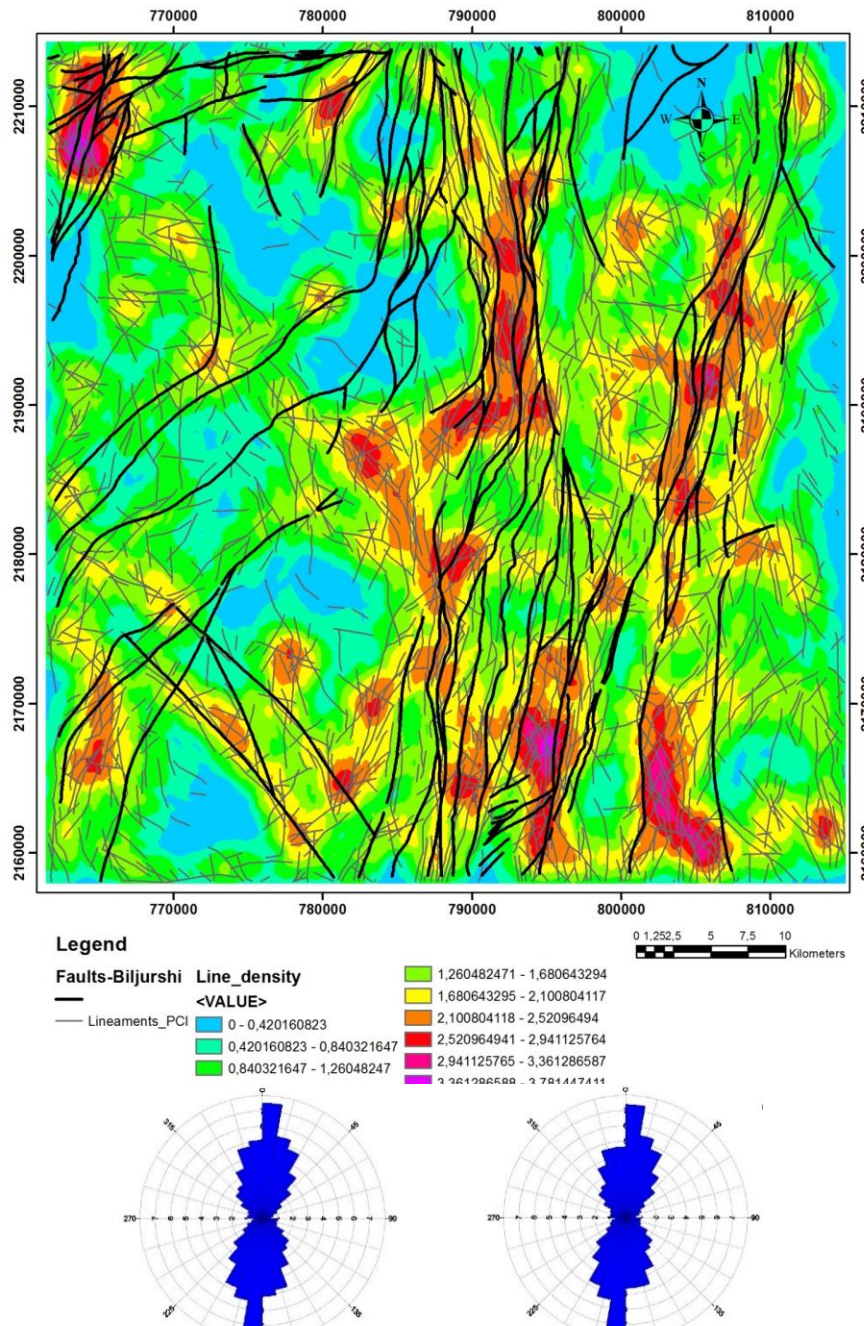
Figure 6. Field faults and Landsat image lineaments over the lineament Density map, and directional rose diagrams based on count (the length to the left; the frequency (number) to the right).

4.3. Lineamentscorrelation

Superposition of results from the image processing with the field geological map,made by [11], highlights a reconciliation of some characteristic parameters and a difference between others (Figure 7). The frequency and length ratio is closely related to the fracture length (segment). The comparison highlights a similarity between the principal directions of lineament resulting from the processed satellite image and the main directional families recognized on the geological map, as well as the appearance of the new directional families by the satellite image (Figure 7).

The geophysical and image lineament maps highlight and locate oriented fault zones in the study area. Many of these zones were showed in outcrop, the others are not known from literature. The remote sensing technique constitutes a good tool for recognized and characterized in direction and length faults that do not appear in the field map(Figure 7). The lineament map represents the principal directional families recognized on the geological map, with some exaggeration in frequency and length. Indeed, the three principal directions N-S to (NNE-SSW, NNW-SSE), NE-SW and NW-SE found on the rose diagrams resulting from the geological map are better represented on that resulted from satellite image (Figure 7). This low representation of directions on

the geological map can be related to the superposition of the direction of geological layer with the fracture directions or simply to the chosen scale for the field mapping. It may also be related to the effect of the terrain accessibility and visibility that prevents a detailed mapping of fractures. However, The NNW-SSE direction observed in the lineament maps is not clearly highlighted on the Biljurshi field fault map except some segments. These lineaments are also showed in the rose diagrams as the second-order dominant direction.
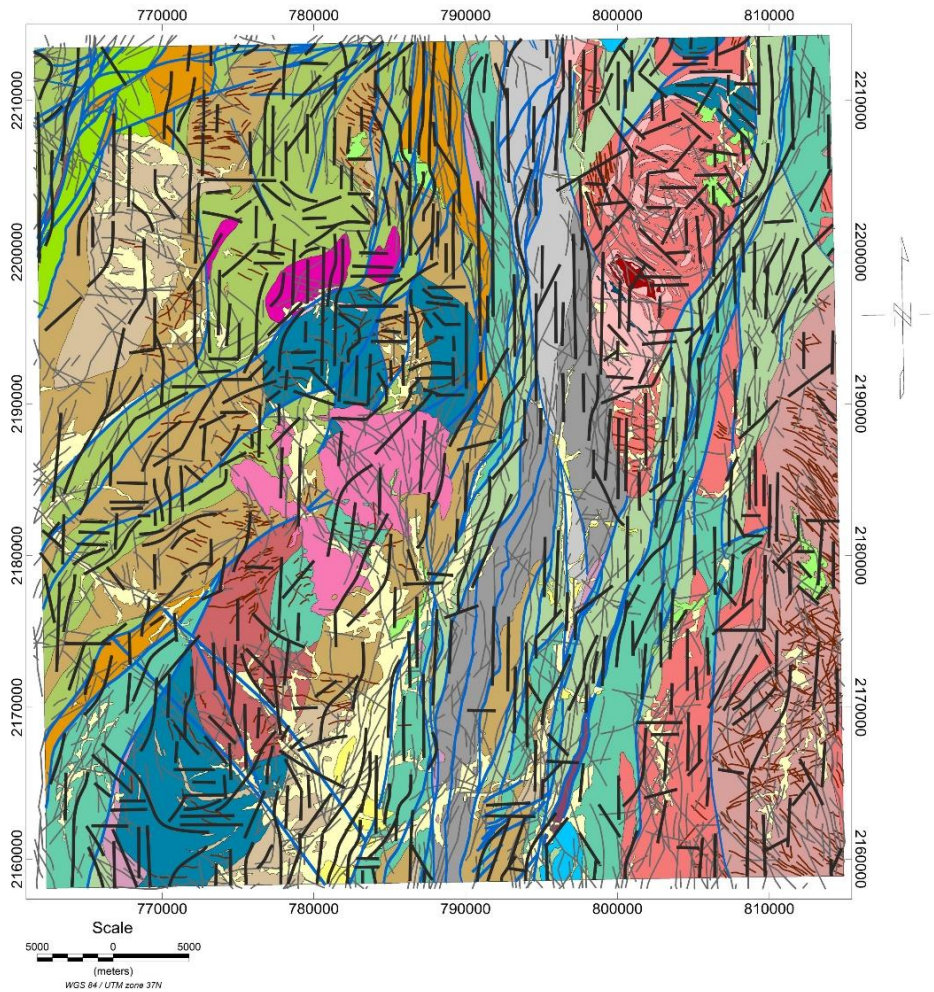
Figure 7. Synthetic structural map generated from integration of field faults (thick blue lines), dikes (thin brown thin lines), and geophysical (thick black lines) and satellite (thin gray lines) lineaments.

V.   Discussion: mineral interests
5.1. Mineralization related to lineaments intersection

Relationship between lineaments and mineralization is to compare the position of lineament intersections with distribution of mineral indices and mines in the study area (Figure 8). The lineaments intersectionallows us to add spatial data to this study. The intersection points could be interpreted as hydrothermal conduits assuming that the majority of secant and training lineaments are faults. The spatial distribution of these zones of strong intersection indirectly informs us about the porosity of hydrothermal paleo-systems and hence of zones favorable for mineralization.
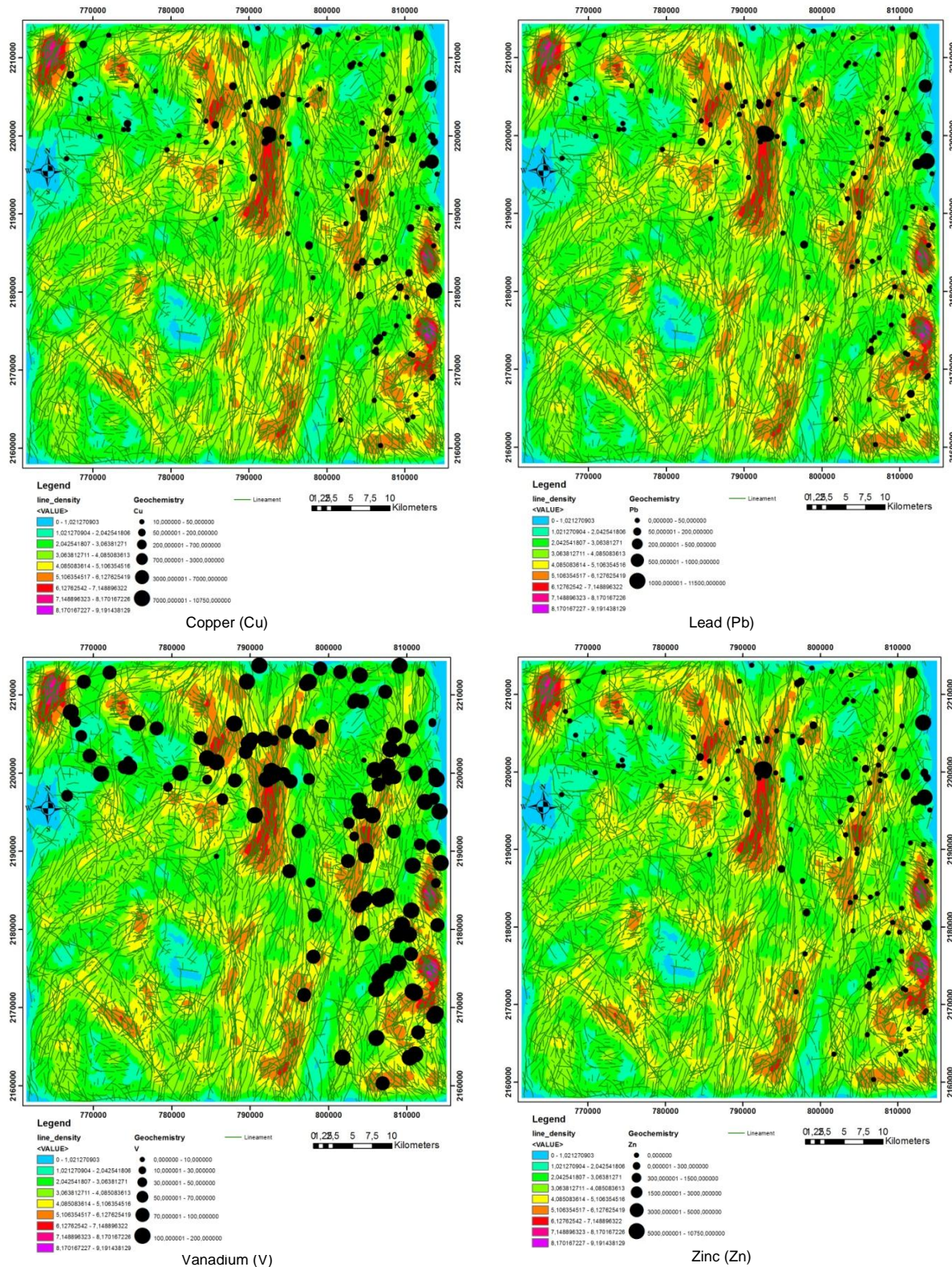
Figure 8. Distribution of content of four main elements, in parts per million (ppm), on the density map of lineament intersections showing position of mineralization compared to the lineament intersection.

The various geochemical elements are mainly located in the volcanosedimentary and metamorphic bands, along the Umm Farwah fault corridor, and in nearby zones, marked by melange of volcano-sedimentary layers and plutonic intrusions. Superimposition of geochemical data on the synthetic map obtained from

geophysical lineaments, satellite imagery and field fault, shows a certain correlation between the mineralization rate and the high density zones of lineaments intersection (Figure 8).

Figure 8 shows the spatial distribution of all intersection points between the N-S, NNE-SSW and NNW-SSE main secant lineament families, as well as with the drag lineaments. As has been demonstrated in the study on the proximity of mineralization around lineaments, the N-S and NNE families seem to have an influence on the mineralization and are, therefore, the most solicited zones.

5.2. Structural and mining aspects

Concerning the geological architecture, this work confirms the structural directions observed on the field. The main geological units are identifiedby magnetic reduced to the pole, and faults are very consistent with the magnetic gradient contours and satellite image. N-S and NNE-SSW dominant directions characterize the Umm Farwah fault system, along the Ablah volcano-sedimentary group.

Moreover, the magnetic and image lineaments showed strong anomalies approximately the existing mines. These anomalies are comparable with those identified in other localities in the study area. This observation could serve as a basis for the sector's exploration strategy. In fact, each anomaly of similar intensity and shape to that located at sites of mining interest, with a similar tectonic context, could be of interest and therefore considered as a prospect area.Furthermore, the resulted structural zones map reveals more faults/lineaments, which indicate that more work, need to be done on these structures to see whether they host other not yet discovered sulfides.

VI. Conclusions

In the present work, we use integrate published field observations with airborne magnetic and satellite data in the Biljurshi area. In order to accomplish the main objectives of the research work, literature review of the previous works was used for summarizing the regional geology including lithology, structures, tectonic deformations and zones of mineralization interests. Airborne geophysical, satellite image, and geochemical data were integrated in order to propose a new map that highlights the geological structures of the basement. The Biljurshi area reveals the presence of a principal near N-S (N-S, NNE-SSW and NNW-SSE) lineaments, with minor NE-SW and NW-SE trending lineaments. Aeromagnetic gradients and Landsat image lineamentshelp in location of potential mineral zones.

The delineated structures control the identified anomalous mineralization zones of the studied area. The northeastern and central-eastern parts of the Biljurshi area remain the most favorable zones for exploration. However, exploration in these areas is not simple because the enclave deposits are to be found in dioriticand gabbroic intrusive complexes and in volcano-sedimentary layers. Under these conditions, and in the presence of geological observations and geochemical indicators proximal and distal compared to the fault positions, geophysics and satellite image are of interest for exploration of theBiljurshi area.

This study allowed the development of potential targets at mineralized sites. Due to the obtained results, a more detailed geochemical work with the execution of exploration drilling is recommended in the zones already mineralized and those discovered by geophysics and remote sensing. Moreover, it should be noted that the absence of the mineralization in outcrop does not mean the absence of deposit because this latter can be deeper than the depths of targeted investigations. Thus, targets of greater depth than those targeted so far may therefore exist.

References

[1]. Shackleton, R.M. (1986). Precambrian collision tectonics in Africa. In: Coward, M.P., and Ries, A.C. (eds.) Collision Tectonics. Geological Society, London, Special Publications, 19, 329-349.
[2]. Shackleton, R.M. (1996). The final collision zone between East and West Gondwana: Where is it?. J. Afr. Earth Sci., 23, 271-287.
[3]. Genna, A., P. Nehlig, E. Le Goff, C. Guerrot and M. Shanti (2002). Proterozoic tectonism of the Arabian Shield. Precambrian Research, 117, 21–40.
[4]. Johnson, P.R. (2006). Explanatory notes to the map of Proterozoic geology of western Saudi Arabia. Saudi Geological Survey, Technical Report SGS, 62.
[5]. Stoeser, D.B. and J.S. Stacey (1988). Evolution, U-Pb geochronology and isotope geology of the Panafrican Nabitah orogenic belt of the Saudi Arabian Shield. In: El-Gaby, S. and R.O. Greiling (Eds.). The Pan-African Belt of Northeast Africa and Adjacent Areas. Vieweg, Braunschweig/Wiesbaden, 227-288.
[6]. Stern, R.J. and P.R. Johnson (2010). Continental lithosphere of the Arabian Plate: A geologic, petrologic and geophysical synthesis. Earth-Sci. Rev., 101, 29–67.
[7]. Greenwood, W.R., D.B. Stoeser, R.J. Fleck and J.S. Stacey (1982). Late Proterozoic island-arc complexes and tectonic belts in the southern part of the Arabian shield, Kingdom of Saudi Arabia. Saudi Arabian Deputy Ministry for Mineral Resources, Open-File Report USGS-OF-02–8, 46.
[8]. Johnson, P.R. and F.H. Kattan (2001). Oblique sinistral transpression in the Arabian shield: the timing and kinematics of a Neoproterozoic suture zone. Precambrian Res., 107, 117-138.
[9]. Johnson, P.R., F.H. Kattan and J.L. Wooden (2001). Implications of SHRIMP and microstructural data on the age and kinematics of shearing in the Asir terrane, southern Arabian shield, Saudi Arabia. Gondwana Res., 4, 172-173.

[10]. Zouaghi, T., E. Aboud and El-S.K. El-Sawy (2019). Aeromagnetic constraints on the structural framework of Umm Farwah fault system and associated neoproterozoic accretion domains of the Asir terrane; the Biljurshi area, Arabian Shield. Ann. Geophys., 62, 5, GM569, 2019; doi: 10.4401/ag-8022

[11]. Greenwood, W.R. (1975a). Geology of the Biljurshi quadrangle, sheet 19/41 B, Kingdom of Saudi Arabia; with a section on geophysical investigation, by G.E. Andreasen; geochemical investigation and mineral resources, by V.A. Trent and T.H. Kiilsgaard. Saudi Arabian Directorate General of Mineral Resources (DGMR), Geologic Map GM-25, 31, scale 1:100 000.

[12]. Prinz, W.C. (1983). Geologic map of the Al Qunfudhah quadrangle, sheet 19E, kingdom of Saudi Arabia. Saudi Arabian Deputy Ministry for Mineral Resources, Geologic Map GM-70 C, 19, scale 1:250 000.

[13]. Stern, R.J. and P.R. Johnson (2010). Continental lithosphere of the Arabian Plate: A geologic, petrologic and geophysical synthesis. Earth-Sci. Rev., 101, 29–67.

[14]. Collenette, P. and D.J. Grainger (1994). Mineral Resources of Saudi Arabia, not including Oil, Natural Gas, and Sulfur. Saudi Arabian Directorate General of Mineral Resources (DGMR), Special Publication, SP-2, 322.

[15]. Johnson, P.R., A. Andresen, A.S. Collins, A.R. Fowler, H. Fritz, W. Ghebreab, T. Kusky and R.J. Stern (2011). Late Cryogenian–Ediacaran history of the Arabian–Nubian Shield: A review of depositional, plutonic, structural, and tectonic events in the closing stages of the northern East African Orogen. J. Afr. Earth Sci., 61, 167–232.

[16]. Greenwood, W.R., R.O. Jackson and P.R. Johnson (1986). Geologic map of the Jabal Al Hasir quadrangle, sheet 19F, Kingdom of Saudi Arabia. Saudi Arabian Deputy Ministry for Mineral Resources, Geoscience Map GM 94C, 31, scale 1:250 000.

[17]. Moufti, M.R.H. (2001). Age, geochemistry, and origin of peraluminous A-type granitoids of the Ablah–Shuwas pluton, Ablah graben Arabian shield. ActaMineralogica–Petrographica, Szeged, 42, 5–20.

[18]. Nehlig, P., A. Genna, F. Asfirane, N. Dubreuil, C. Guerrot, J.M. Eberlé, H.M. Kluyver, J.L. Lasserre, E. Le Goff, N. Nicol, N. Salpeteur, M. Shanti, D. Thiéblemont and C. Truffert (2002). A review of the Pan-African evolution of the Arabian Shield. GeoArabia, 7 (1), 103-124.

[19]. Anderson, R.E. (1977). Geology of the Wadi Tarj Quadrangle, Sheet 19/42 A, Kingdom of Saudi Arabia. Saudi Arabian Directorate General of Mineral Resources (DGMR), Geologic Map GM-24, 24, Scale 1:100 000.

[20]. Bhattacharyya, B.K. (1965). Two-dimensional harmonic analysis as a tool for magnetic interpretation. Geophys., 30, 829-857.

[21]. Spector, A. and F.S. Grant (1970). Statistical models for interpreting aeromagnetic data. Geophys., 35 (2), 293-302.

[22]. Parker, R.L. (1972). The rapid calculation of potential anomalies. Geophysical Journal of the Royal Astronomical Society 31, 447-455.

[23]. Baranov, W. (1975). Potential fields and their transformations in applied geophysics. Geoexploration monographs Series, serie 1, n°6. Gebrüder Borntraeger - Berlin - Stuttgart (Ed), 121 pp.

[24]. Gunn, P.J. (1975). Linear transformations of gravity and magnetic fields. Geophysical Prospecting 23, 300-312.

[25]. Parker, M. (1992). Using older geophysical surveys: Problems and solutions. ESAMRDC report 92/TECH/74, 22p.

[26]. Sabins, F.F. (1996). Remote Sensing: Principles and Interpretation, 3rd Ed.: W. H. Freeman and Company. New York, 494 p.